



we show that the absolute value of  ${}_0D_t^q \text{sgn}(e)$  can be greater than 1 (i.e.  $|\text{sgn}(e)|$  is just limited at 0 or 1). This is the second important property of the FO sign function.

Based on  ${}_0D_t^q \text{sgn}(e)$ , an FO SM-ESC is proposed for the optimization of nonlinear systems. In the FO SM-ESC, the first property of  ${}_0D_t^q \text{sgn}(e)$ ,  $0 \leq q < 1$  guarantees that the output achieves an arbitrary small neighborhood of the optimal operational point and remains close to it thereafter. The second property can improve the control performance (i.e. convergence speed and accuracy). The changes of  ${}_0D_t^q \text{sgn}(e)$ ,  $0 \leq q < 1$  with respect to  $q$  and  $t$  are visualized to show how the properties of the FO sign function contribute to the superior tracking behavior. Further FO/IO SM-ESC comparisons are given. They show the advantage of the FO SM-ESC over the IO SM-ESC clearly. Both simulation and experimental results demonstrate the advantages of the designed control scheme.

**2. Fractional-order sliding mode based extremum seeking control**

**2.1. Problem formulation**

Consider a single-input–single-output (SISO) nonlinear system (Krstić & Wang, 2000; Pan et al., 2003)

$$\frac{d}{dt}x = f(x, u), \tag{1}$$

$$y = \tilde{F}(x), \tag{2}$$

where  $x \in R^n$ ,  $u \in R$ ,  $y \in R$  are respectively the state, control input and output.  $f(x, u)$  and  $\tilde{F}(x)$  are smooth. Without loss of generality, we consider the maximization of  $y$ . We do not assume the knowledge of  $\tilde{F}(\cdot)$ . Consider a smooth control law:  $u = \eta(x, \theta)$ , parameterized by a scalar parameter  $\theta$ . The system (1) is derived as  $\frac{d}{dt}x = f(x, \eta(x, \theta))$ .

**Assumption 1.**  $\exists$  a smooth function  $x_e : R \rightarrow R^n$  such that  $f(x, \eta(x, \theta)) = 0$  if and only if  $x = x_e(\theta)$ .

**Assumption 2.** At the equilibrium point  $x_e(\theta)$ , the static performance map from  $\theta$  to  $y$  (i.e.  $y(t) = \tilde{F}(x_e(\theta)) = F(\theta)$ ) is smooth.

We suppose that there exists a unique maximum at  $\theta^*$  for  $F(\theta)$ .  $\theta^*$ ,  $F(\cdot)$  and its gradient for any  $\theta$  are assumed to be unknown to the control designer. By utilizing  $F'(\theta) = dF(\theta)/d\theta$ ,  $F''(\theta) = d^2F(\theta)/d\theta^2$ , one has  $\frac{d}{dt}y = F'(\theta)\frac{d}{dt}\theta$ . The following assumption is listed.

**Assumption 3.** There exists a unique  $\theta^* \in R$  such that  $F'(\theta^*) = 0$  and  $F''(\theta^*) < 0$ . For any given  $\varepsilon > 0$ , there exists  $\delta = \delta(\varepsilon)$  such that  $|F'(\theta)| > \varepsilon$ ,  $\forall \theta \notin D_\delta$ , where  $D_\delta = \{\theta : |\theta - \theta^*| < \delta/2\}$  is called  $\delta$ -vicinity of  $\theta^*$ .

In order to design an FO SM-ESC, we use the following definition and lemmas.

**Definition 1.** The Riemann–Liouville (RL) definition of the  $q$ th order derivative is Monje, Chen, Vinagre, Xue, and Feliu (2010) and Samko, Kilbas, and Marichev (1993)  ${}_0D_t^q f(t) = \frac{d^q f(t)}{dt^q} = \frac{1}{\Gamma(m-q)} \frac{d^m}{dt^m} \int_0^t \frac{f(\tau)}{(\tau-t)^{q+1-m}} d\tau$ , where  $n-1 < q \leq n$  with  $n$  is the integer,  $\Gamma(\cdot)$  is the gamma function.

**Lemma 1** (Kilbas, Srivastava, & Trujillo, 2006 and Samko et al., 1993). The fractional integration operator  ${}_aI_t^\beta = \frac{1}{\Gamma(\beta)} \int_a^t \frac{f(\tau)}{(\tau-t)^{1-\beta}} d\tau$ , ( $t > a$ ;  $\beta \in C$ ,  $\text{Re}(\beta) > 0$ ) is bounded in  $L_p(\hat{a}, \hat{b})$ , ( $1 \leq p \leq \infty$ ,  $-\infty < \hat{a} < \hat{b} < \infty$ ):

$$\|{}_aI_t^\beta f\|_p \leq K \|f\|_p, \quad \left( K = \frac{\hat{b} - \hat{a}}{\text{Re}(\beta)|\Gamma(\beta)|} \right). \tag{3}$$

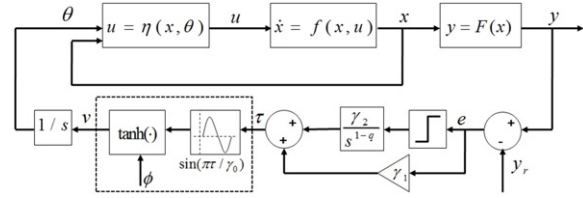


Fig. 1. Block diagram of the proposed FO SM-ESC scheme.

**Lemma 2.** Consider the RL fractional derivative operator  ${}_0D_t^q f(t) = \frac{1}{\Gamma(1-q)} \frac{d}{dt} \int_0^t \frac{f(\tau)}{(\tau-t)^q} d\tau$ ,  $0 \leq q < 1$  and sign function, one can obtain

$${}_0D_t^q \text{sgn}(e(t)) \begin{cases} > 0, & \text{if } e(t) > 0, t > 0, \\ < 0, & \text{if } e(t) < 0, t > 0. \end{cases} \tag{4}$$

**Proof.** See Appendix A.

From Lemma 2,  ${}_0D_t^q \text{sgn}(e)$ ,  $0 \leq q < 1$  is proven to be able to extract the sign of  $e$ . This is its first property.

**Remark 1.** Consider two cases: (1)  $e(t) > 0, \forall t > 0$ , one has  ${}_0D_t^q \text{sgn}(e) = \frac{t^{-q}}{\Gamma(1-q)}$ ; (2)  $e(t) < 0, \forall t > 0$ , one also has  ${}_0D_t^q \text{sgn}(e) = \frac{-t^{-q}}{\Gamma(1-q)}$ . Thus,  ${}_0D_t^q \text{sgn}(e)$  are bounded in both cases. Since the absolute value of the above cases is greater than the other cases,  ${}_0D_t^q \text{sgn}(e)$ ,  $\forall e$  is bounded, i.e. there exists  $\varpi > 0$  such that  $|{}_0D_t^q \text{sgn}(e)| < \varpi$ .

**2.2. FO sliding mode based extremum seeking control**

An FO SM-ESC will be designed for the system (1). First, the tracking error is defined as  $e = y - y_r$ , in which  $\dot{y}_r = k_r$ ,  $y_r(0) = y_{r0}$ , with  $k_r > 0$  and  $y_{r0}$  is a design constant. So as to avoid an unbounded  $y_r(t)$ , one can saturate  $y_r(t)$  at a rough known upper bound of  $y^*$ . Based on  $e$ , a function  $\tau$  is proposed by

$$\tau = \gamma_1 e + \gamma_2 ({}_0D_t^{q-1} \text{sgn}(e)), \tag{5}$$

where  $\gamma_i > 0$ , ( $i = 1, 2$ ),  $0 \leq q < 1$ ,  ${}_0D_t^{q-1}$  is an RL fractional operator. The parameter  $\theta$  is defined to meet  $\dot{\theta} = v$ , in which  $v$  denotes variable structure control

$$v = \phi \tanh \left( \sin \left( \frac{\pi}{\gamma_0} \tau \right) \right), \tag{6}$$

in which  $\phi$  denotes a designed modulation function and  $\gamma_0 > 0$ . The FO SM-ESC is depicted in Fig. 1.

**3. Stability analysis of FO sliding mode based extremum seeking control**

**3.1. Stability analysis of the FO SM-ESC**

First, one has  $\dot{\tau} = \gamma_1 F' v + \xi_s$ , where  $\xi_s := -\gamma_1 k_r + \gamma_2 {}_0D_t^q \text{sgn}(e)$ . Denoting  $k = \gamma_1 F'$ , one has  $\dot{\tau} = k(v + \omega)$ , in which  $\omega := (-\gamma_1 k_r + \gamma_2 {}_0D_t^q \text{sgn}(e))/k$ . From Assumption 3, there exists  $0 < \bar{k} \leq \gamma_1 \varepsilon$  such that  $\bar{k} \leq |k|$ ,  $\forall \theta \notin D_\delta$ .  $\phi$  will be designed such that  $\phi \tanh^2(\sin(\pi \tau / \gamma_0)) \geq |\omega| + \alpha$ , in which  $\alpha \geq 0$ . Hence,  $|\omega| \leq \hat{\omega}$ , where  $\hat{\omega} \leq (\gamma_1 k_r + \gamma_2 \varpi) / \bar{k}$ . Next, one possible  $\phi$  will be proposed to guarantee the control performance.

**Theorem 1.** Consider the system (1)–(2) with the FO SM-ESC (6). Outside the  $D_\delta$ , if  $\phi$  in (6) satisfies

$$\phi \tanh^2(\sin(\pi \tau / \gamma_0)) := [(\gamma_1 k_r + \gamma_2 \varpi) + \|y_r\| e^{-\alpha_1 t}] / \bar{k} + \alpha, \tag{7}$$

where  $\alpha_1 > 0$ , then, while  $\theta \notin D_\delta$ , one has (i): no finite-time escape happens in the closed-loop signals ( $t_M \rightarrow +\infty$ ) and (ii) a sliding mode on  $\tau(t) = l\gamma_0$  is arrived in finite time for some integer  $l$ .

**Proof.** See Appendix B.

Next, it will be shown that the FO SM-ESC with  ${}_0D_t^q \text{sgn}(e)$ ,  $0 \leq q < 1$  and  $\phi$  ensures that  $\theta$  arrives at  $D_\delta$  of the unknown maximizer  $\theta^*$  defined in Assumption 3.

**Theorem 2.** Consider the system (1)–(2) under the controller (6) with the function (7). If Assumptions 1–3 are satisfied, then: (i)  $D_\delta$  in Assumption 3 is globally attractive that is achieved in finite time and (ii) for small enough  $\varepsilon$ , the oscillations around  $y^*$  of  $y$  can be made of order  $O(\gamma_0)$ . Furthermore, all closed-loop system signals are uniformly bounded (UB) except for  $\tau(t)$  that is an argument of an FO sign function in (5).

**Proof.** See Appendix C.

3.2. Comparison between IO SM-ESC and FO SM-ESC

In our previous work Yin et al. (2012), the IO SM-ESC with  $\tanh(\sin(\pi\tau/\gamma_0))$  was developed.  $\tau$  in the IO SM-ESC is given by

$$\tau = \gamma_1 e + \gamma_2 \text{sgn}(e), \tag{8}$$

where  $e = y - y_r$ .  $\theta$  is proposed to satisfy  $\dot{\theta} = v$ , in which  $v = \phi \tanh(\sin(\pi\tau/\gamma_0))$ . The IO SM-ESC can ensure that  $y$  approaches  $y^*$  and stays in it thereafter. Since  ${}_0D_t^q \text{sgn}(e) = \frac{1}{\Gamma(1-q)} \frac{d}{dt} \int_0^t \frac{\text{sgn}(e(\epsilon))}{(t-\epsilon)^q} d\epsilon = \text{sgn}(e)$ , the FO SM-ESC with  ${}_0D_t^q \text{sgn}(e)$ ,  $0 \leq q < 1$  is an FO/IO controller synthesis (IO controller with  $\text{sgn}(e)$  and FO controller with  ${}_0D_t^q \text{sgn}(e)$ ,  $0 < q < 1$ ). In what follows, a comparison and analysis for the FO/IO SM-ESC synthesis reveal the reason the FO SM-ESC can have a better tracking performance.

One property of the good tracking performance is that  $y$  can quickly reach  $y^*$ . In order to show how to obtain a faster tracking performance under the FO SM-ESC, the following remark is presented.

**Remark 2.** The proof of Theorem 1 uses  $\tanh(\sin(\pi\tau/\gamma_0))$  to ensure the existence of a series of sliding surfaces  $s_l = \tau - l\gamma_0$  and realization of  $\tau$ -sliding modes, while  $\theta \notin D_\delta$ . One has  $\dot{e} = -(\gamma_2/\gamma_1) {}_0D_t^q \text{sgn}(e)$  from  $\dot{\tau} = 0$ . From Lemma 2, one has the following relationship (in which  $y(0)$ ,  $y_r(0)$  are the initial conditions of  $y$  and  $y_r$ )

- (I) When  $e(0) = y(0) - y_r(0) < 0$  (i.e.  $y(0) < y_r(0)$ ), one has  $e \nearrow$  since  $\dot{e} = -(\gamma_2/\gamma_1) {}_0D_t^q \text{sgn}(e) > 0$ , then,  $y$  will be close to  $y_r$ .
- (II) When  $e(0) = y(0) - y_r(0) > 0$  (i.e.  $y(0) > y_r(0)$ ), one has  $e \searrow$  since  $\dot{e} = -(\gamma_2/\gamma_1) {}_0D_t^q \text{sgn}(e) < 0$ , then,  $y$  will be close to  $y_r$ .

Hence, outside a small  $\gamma_0$ -neighborhood of  $y^*$ ,  $y$  tries to track  $y_r$ . One can assure that  $y$  approaches  $y^*$ . Moreover, it is more likely to choose a series of  $q$ , ( $0 < q < 1$ ) such that  $|{}_0D_t^q \text{sgn}(e)|$  is bigger than 1 (i.e.,  $|{}_0D_t^q \text{sgn}(e)| \gg 1 = |\text{sgn}(e)|$ ) during the initial time interval. This is the second important property of  ${}_0D_t^q \text{sgn}(e)$  where  $y$  determined by the FO SM-ESC will create a stronger push to any arbitrary small vicinity of  $y^*$  during this time interval, even if  $|{}_0D_t^q \text{sgn}(e)| \leq 1$  during the next time interval. The simulation and experimental results in Section 5 can help to demonstrate the advantages of the FO SM-ESC.

**Remark 3.** Especially, the maximum point of some systems (e.g. MPPT of the PV plant Malek et al., 2012) may be constantly changing with environmental variations, but the rough upper bound of the maximum point is known.  $y_{r0}$  can be chosen such that  $y_{r0}$  is bigger than the upper bound, such that  $y_r$  can draw  $y$  close to  $y^*$  and  $e < 0$ . Thus,  $y$  with the positive rate  $\dot{y} = k_r - (\gamma_2/\gamma_1) {}_0D_t^q \text{sgn}(e)$

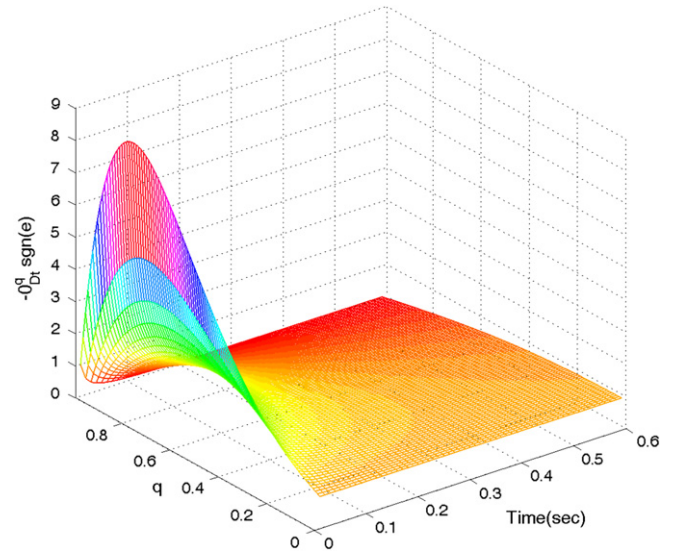


Fig. 2. Relationship between  ${}_0D_t^q \text{sgn}(e)$  and  $q$ , for  $e(t) < 0$ ,  $0 \leq q < 1$ .

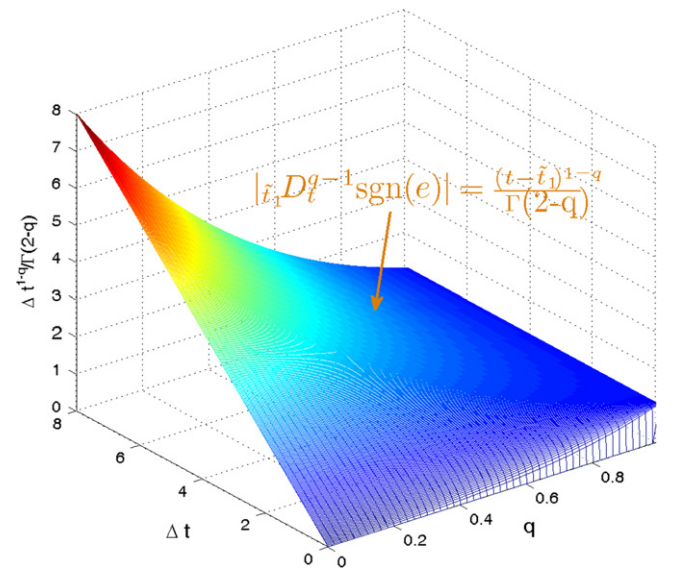


Fig. 3. Relationship between  $\Delta t^{1-q}/\Gamma(2-q)$  and  $q$ , for  $e(t) < 0$ ,  $0 \leq q < 1$ .

approaches  $y^*$  when  $y$  is out of the  $\gamma_0$  vicinity of  $y^*$ . Similarly, the rate of  $y$  under the IO SM-ESC is  $k_r + \gamma_2/\gamma_1$ . As shown in Fig. 2,  $-{}_0D_t^q \text{sgn}(e) \gg 1 = -\text{sgn}(e)$ ,  $0 < q < 1$  during the initial time interval. Thus,  $k_r - (\gamma_2/\gamma_1) {}_0D_t^q \text{sgn}(e) > k_r + \gamma_2/\gamma_1$  in the time interval. One can assure that the FO SM-ESC with  $0 < q < 1$  has a faster tracking performance than that the IO SM-ESC does. The MPPT of the PV model in Section 4 shows the advantages of the FO SM-ESC.

Another property of the good tracking performance is to drive towards a smaller neighborhood of  $y^*$ . The following remark illustrates the reason the oscillations under the FO SM-ESC can be reduced.

**Remark 4.** In Theorem 2, the oscillations around  $y^*$  of  $y$  can be made of order  $O(\gamma_0)$ . Now, we consider  ${}_t D_t^{q-1} \text{sgn}(e)$  in (C.1). Since  $e(t) < 0$ ,  $\forall t > \tilde{t}_1$ , one has  $|{}_t D_t^{q-1} \text{sgn}(e)| = \frac{(t-\tilde{t}_1)^{1-q}}{\Gamma(2-q)}$ . From (C.1), one has

$$|\tilde{y}(t)| \leq \gamma_1 |\tilde{\tau}(t)| + \gamma_1 k_r (t - \tilde{t}_1) + \frac{\gamma_2}{\Gamma(2-q)} (t - \tilde{t}_1)^{1-q},$$



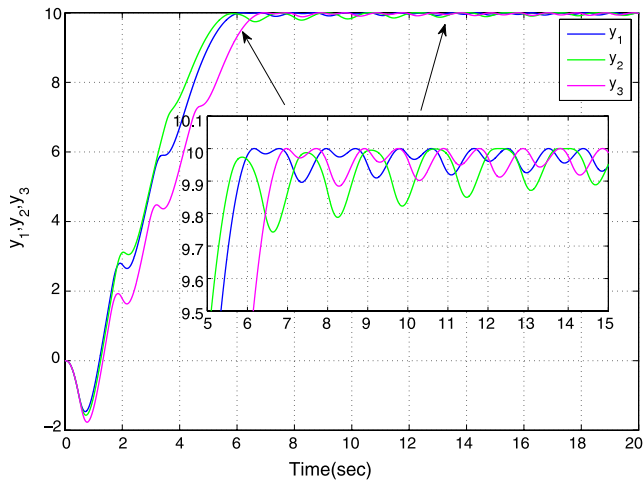


**Fig. 4.** Time responses of  $y_1$  (blue line) under the FO SM-ESC,  $y_2$  (green line) under the IO SM-ESC in Oliveira et al. (2011) and  $y_3$  (purple line) under the IO SM-ESC in Pan et al. (2003). (For interpretation of the references to color in this figure legend, the reader is referred to the web version of this article.)

$\forall t > \tilde{t}_1$ . Similarly, one has  $|\tilde{y}(t)| \leq \gamma_1 |\tilde{\tau}(t)| + \gamma_1 k_r (t - \tilde{t}_1) + \gamma_2 (t - \tilde{t}_1)$ ,  $\forall t > \tilde{t}_1$  by using the IO SM-ESC. Since  $t - \tilde{t}_1 = \frac{(t - \tilde{t}_1)}{\Gamma(2)}$ , it is more likely for the FO SM-ESC to obtain a smaller vicinity of  $y^*$ . Denoting  $\Delta t = t - \tilde{t}_1$ ,  $t > \tilde{t}_1$ , the changes in  $-\frac{\Delta t^{1-q}}{\Gamma(2-q)}$ , with different  $q$  and  $\Delta t$ , in which  $q \in [0, 0.99]$ ,  $\Delta t \in [0, 8]$  are depicted in Fig. 3. Since there exist many  $q, t$  such that  $0 < \frac{1}{\Gamma(2-q)}(t - \tilde{t}_1)^{1-q} < t - \tilde{t}_1$ , the oscillations around  $y^*$  of  $y$  under the FO SM-ESC can be made smaller.

**4. Simulation and experimental results**

**4.1. Simulation results**

In this subsection, two examples are used to illustrate the effectiveness of the proposed FO SM-ESC scheme.

**Example 1.** Consider the double-integrator system (Pan et al., 2003)

$$\begin{cases} \dot{x}_1 = x_2, \\ \dot{x}_2 = u, \end{cases} \quad (9)$$

with  $u(t) = -30(x_1(t) - \theta(t)) - 11x_2(t)$  and the output  $y(t) = -10(x_1(t) - 5)^2 + 10$ .  $y(t)$  reaches its maximum  $y^* = 10$  at  $x_1(t) = 5$ .  $x_1(0) = \theta(0) = 4$ ,  $x_2(0) = y_r(0) = 0$  and  $k_r = \gamma_0 = \gamma_1 = 2$ ,  $\phi = 0.25$  are chosen, the same as in Pan et al. (2003).  $\gamma_1 = 0.5$  is selected in the simulation. Fig. 4 shows the comparison of  $y_1$  under the FO SM-ESC with  $q = 0.4$ ,  $y_2$  under the IO SM-ESC law in Oliveira, Hsu, and Peixoto (2011) and  $y_3$  under the IO SM-ESC in Pan et al. (2003). It shows that  $y_1$  has faster tracking performance and higher accuracy than  $y_2, y_3$ .

Next, the simulations are performed while  $q$  is changed. Fig. 5 shows that  $y_1, y_3$  under the FO SM-ESC with  $q_1 = 0.5, q_3 = 0.2$  arrive at  $y^*$  more rapidly than  $y_2$  under the IO SM-ESC, since  $|{}_0D_t^{0.5} \text{sgn}(e)| \gg 1, |{}_0D_t^{0.3} \text{sgn}(e)| \gg 1$  during  $[0, 0.4]$ . Furthermore,  $y_1$  and  $y_3$  achieve to a smaller vicinity of  $y^*$  than  $y_2$  does. Thus, the FO SM-ESC can have better tracking performance.

**Example 2.** Consider the MPPT problem of a PV array. In the PV system, the net current of the cell is the difference of the photocurrent  $I_L$  and the normal diode current  $I_0$ :  $I = I_L - I_0 \left( e^{\frac{q(V+IR_s)}{nKT}} - 1 \right)$ , that  $I, V$  are the current and voltage,  $n$  denotes a variable parameter (instead of being fixed at either 1 or 2). We consider the model in Malek et al. (2012) and Walker (2001). The PV module provides about 48 W of nominal maximum power, when  $T = 25^\circ$  and  $G = 1000 \text{ W/m}^2$ . Then, we describe the design of the proposed MPP. Consider the following auxiliary first order nonlinear system:

$$\dot{V} = v, \quad I = h(V) = I_L - I_0 \left( e^{\frac{q(V+IR_s)}{nKT}} - 1 \right). \quad (10)$$

To maximize the power output  $P = VI$ , we employ the FO SM-ESC (6) with  $q = 0.1$  for (10). Matlab s-function is used to express the PV model, adopted from Walker (2001).  $\phi = (\gamma_1 + \gamma_2 + \gamma_1 k_r) / \varepsilon + \alpha$  and  $\varepsilon = 0.1\gamma_0$  are used. Let  $V(0) = 0, y_r(0) = 50$  and  $\gamma_0 = 0.01, \gamma_1 = 0.5, \gamma_2 = 0.1, k_r = 0.5$  and  $\alpha = 0.1$  in our simulations. Fig. 6 shows the comparison between  $P_1$  under the FO SM-ESC and  $P_2$  under the IO SM-ESC. It shows that  $P_1$  converges to the MPP faster than  $P_2$ . Moreover, the amplitude of the oscillations around  $P_{MPP}$  of  $P$  can be reduced by utilizing the FO SM-ESC.

Next, the simulations are done while  $q$  is changed. Since  $|{}_0D_t^{0.17} \text{sgn}(e)|, |{}_0D_t^{0.25} \text{sgn}(e)|, |{}_0D_t^{0.4} \text{sgn}(e)|$  are bigger than 1 during  $[0, 0.2]$ ,  $P_{FO-SM-ESC}$  reaches  $P^*$  than  $P_{IO-SM-ESC}$ , as shown in Fig. 7. They show the advantage of the FO SM-ESC.

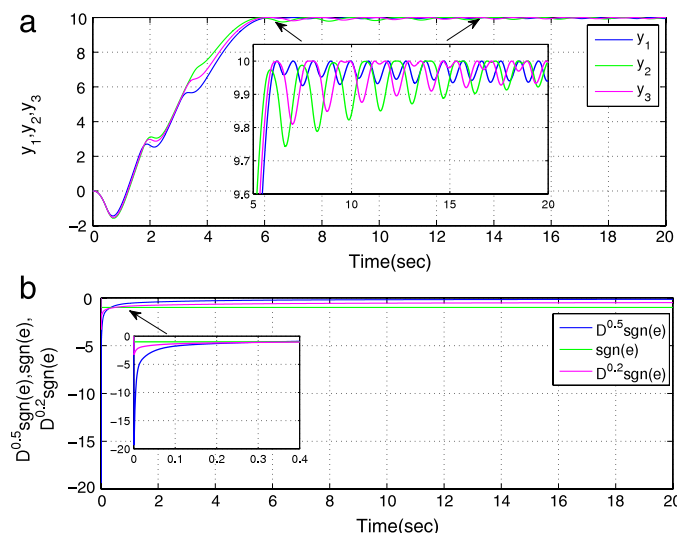


**Fig. 5.** (a) Time responses of  $y_1$  (blue line) and  $y_3$  (purple line) under the FO SM-ESC with  $q_1 = 0.5, q_3 = 0.3$  and  $y_2$  (green line) under the IO SM-ESC in Oliveira et al. (2011); (b) time responses of  $D^{0.5} \text{sgn}(e), D^{0.3} \text{sgn}(e)$  and  $\text{sgn}(e)$ . (For interpretation of the references to color in this figure legend, the reader is referred to the web version of this article.)

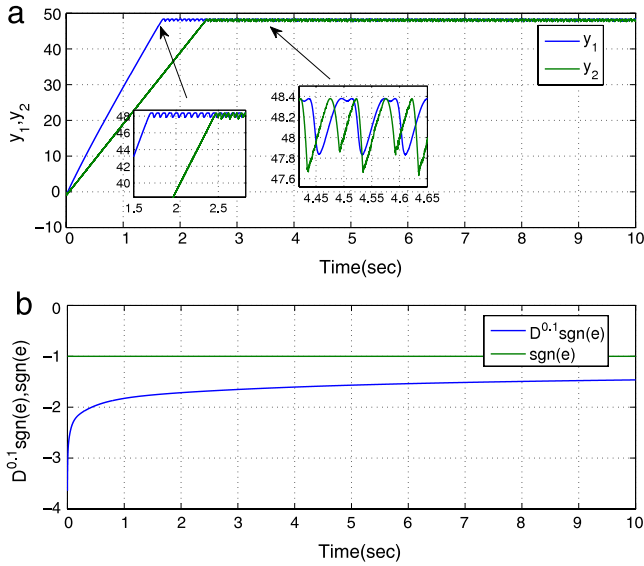


Fig. 6. (a) Time responses of  $P_1$  (blue line) under our control and  $P_2$  (green line) under the IO SM-ESC law in Oliveira et al. (2011); (b) time responses of  ${}_0D_t^{0.1} \text{sgn}(e)$  and  $\text{sgn}(e)$ . (For interpretation of the references to color in this figure legend, the reader is referred to the web version of this article.)

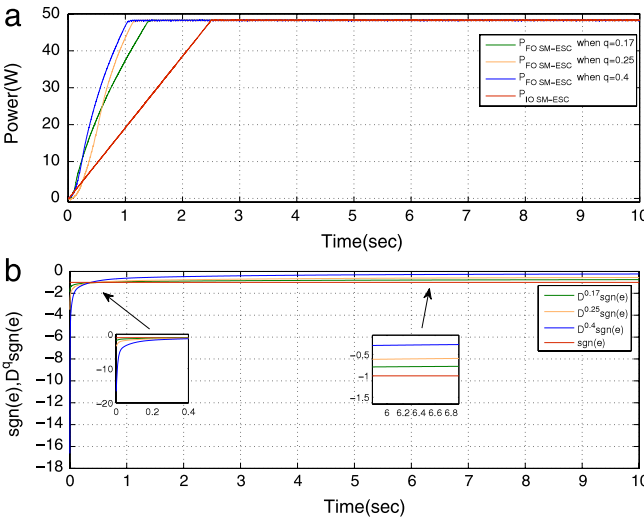


Fig. 7. (a) Time responses of  $P_i$ , ( $i = 1, 2, 3, 4$ ) for different fractional orders; (b) time responses of  ${}_0D_t^{0.17} \text{sgn}(e)$ ,  ${}_0D_t^{0.25} \text{sgn}(e)$ ,  ${}_0D_t^{0.4} \text{sgn}(e)$  and  $\text{sgn}(e)$ .

4.2. Experimental results

A fractional horsepower dynamometer has been applied to model the PV model in Malek et al. (2012). In Fig. 8, the dynamometer (Tarte, Chen, Ren, & Moore, 2006) has a DC motor, an optical encoder, a hysteresis brake, a load cell, and a tachometer. It communicates with a Quanser Q4 terminal board for the connect with the Matlab/Simulink Real-Time Workshop environment by WinCon 4.0. The DC motor is identified

$$G_m(s) = \frac{1.52}{1.01s + 1} \tag{11}$$

In Malek et al. (2012), the PV panel has been built by the hysteresis brake. The break output torque is considered as output current of PV modules. Thus, the power is a product of the angular velocity and the current of PV modules. The proposed scheme is given in Fig. 9. The brake and motor are separately driven by an advanced motion controls brush type PWM servo amplifier Model 50A8. These controllers obtain analog signals from data acquisition

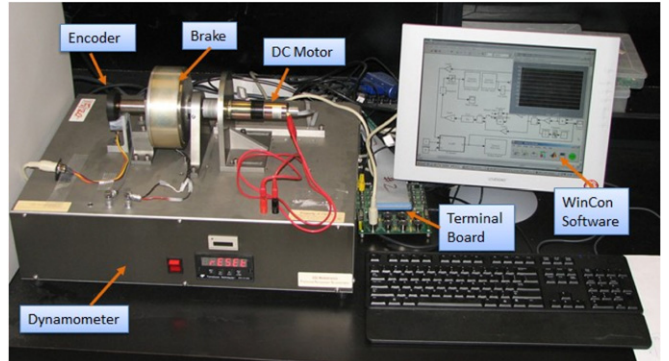


Fig. 8. The fractional horsepower dynamometer.

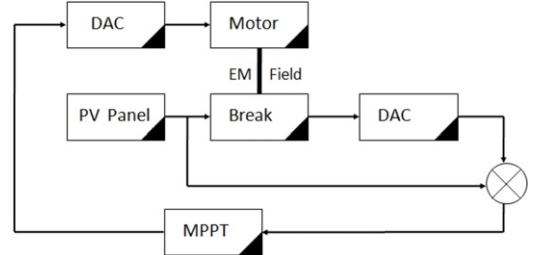


Fig. 9. Modeling the PV panel using the fractional horsepower dynamometer.

hardware. The PWM controllers use the signals to set the voltage output to the motor or the brake.

In this experiment, the FO SM-ESC is applied to the dynamometer as the PV model. The Simulink model used for the experiment is shown in Fig. 10. The comparison between the FO/IO SM-ESC for PV model is depicted in Figs. 11-12. Fig. 11(a) shows the comparison of  $P_i$ , ( $i = 0, 1, 2, 3, 4$ ) under the FO SM-ESC with  $q_0 = 0$ ,  $q_1 = 0.1$ ,  $q_2 = 0.2$ ,  $q_3 = 0.35$ ,  $q_4 = 0.42$ . Fig. 11(b) shows the comparison between  $\text{sgn}(e)$  and  ${}_0D_t^{q_i} \text{sgn}(e)$  with  $q_i$ , ( $i = 1, 2, 3, 4$ ). As shown in Fig. 11, since  $|{}_0D_t^{q_i} \text{sgn}(e)| \gg 1$ ,  $i = 1, 2, 3, 4$  during  $[0, 0.05]$ ,  $P_i$ , ( $i = 1, 2, 3, 4$ ) with the faster convergence speed achieve to the  $\gamma_0$ -neighborhood of  $P^*$  when compared to  $P_0$ . The corresponding  $V_i$  and  $J_i$ , ( $i = 0, 1, 2, 3, 4$ ) are depicted in Fig. 12(a) and (b), respectively. They show that the FO SM-ESC has a better tracking performance.

5. Conclusion

In this paper, the FO SM-ESC law with  ${}_0D_t^q \text{sgn}(e)$ ,  $0 \leq q < 1$  was proposed for the optimization of nonlinear systems. The FO SM-ESC was developed by combining the FO sign function and the tanh periodic switching function. It has been shown that the FO sign function can help to own faster convergence to an arbitrary smaller vicinity of the optimal point, when compared to the sign function. Simulation and experimental results show the advantages of the proposed FO control scheme.

Appendix A. Proof of Lemma 2

For  $\forall t > 0$ , there exists a time series  $\{t_i\}$  in which  $t_0 = 0$ ,  $t_{j_1} > t_{j_2}$  (when  $j_1 > j_2$ ,  $\forall j_1, j_2 \in N$ ) such that  $t \in (t_k, t_{k+1}]$ ,  $\exists k \in N$  and  $e(t') \leq 0$ ,  $\forall t' \in (t_i, t_{i+1}]$ , if  $e(t) \geq 0$ ,  $\forall t' \in (t_{i-1}, t_i]$  when  $i < k$ . Moreover, we require  $e(\bar{t}) \neq 0$ , where  $\bar{t}$  is the first time in  $(t_i, t_{i+1})$ . Thus, the details can be divided into two cases: (a) while  $e(t') \geq 0$ ,  $\forall t' \in (t_0, t_1]$ ,  $e(t') \leq 0$ ,  $\forall t' \in (t_1, t_2]$ , and then,  $e(t') \geq 0$ ,  $\forall t' \in (t_2, t_3]$ , and so on. (b) While  $e(t') \leq 0$ ,  $\forall t' \in (t_0, t_1]$ ,  $e(t') \geq 0$ ,  $\forall t' \in (t_1, t_2]$ , and then,  $e(t') \leq 0$ ,  $\forall t' \in (t_2, t_3]$ , and so on.

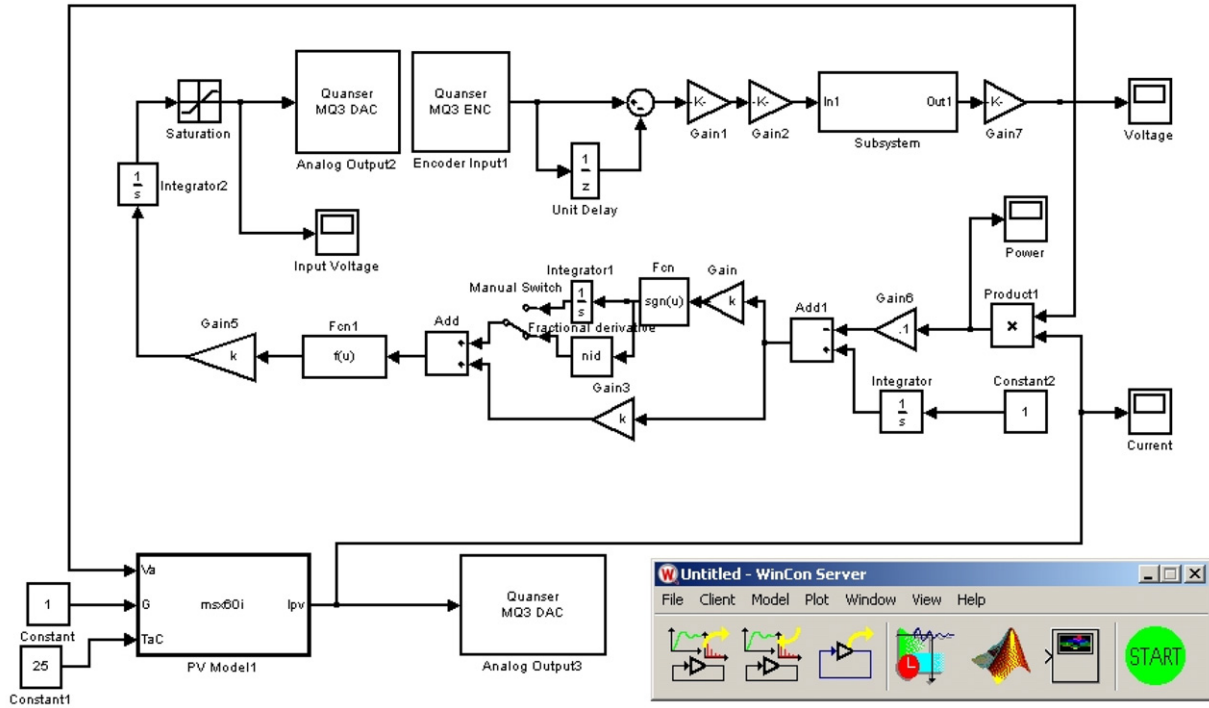


Fig. 10. Simulink model used in the FO SM-ESC real time experiment using RTW Windows Target.

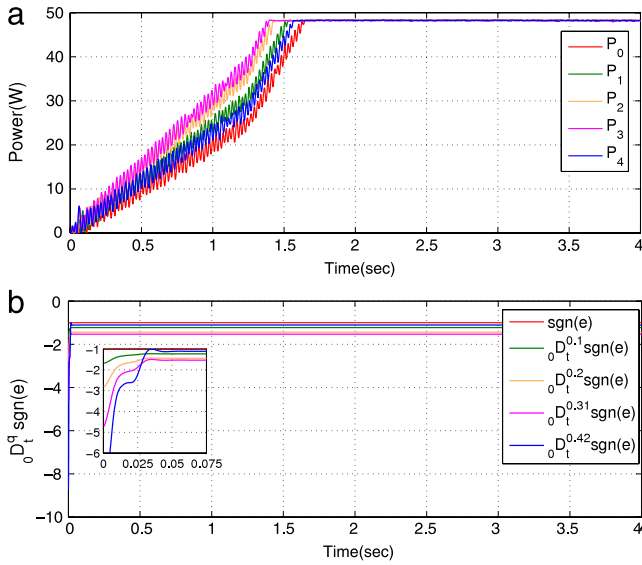


Fig. 11. (a)  $P_i$ ,  $i = 1, 2, 3, 4$  under the FO SM-ESC and  $P_0$  under the IO SM-ESC; (b) time histories of  ${}_0D_t^{0.1}\text{sgn}(e)$ ,  ${}_0D_t^{0.2}\text{sgn}(e)$ ,  ${}_0D_t^{0.31}\text{sgn}(e)$ ,  ${}_0D_t^{0.42}\text{sgn}(e)$  and  $\text{sgn}(e)$ .

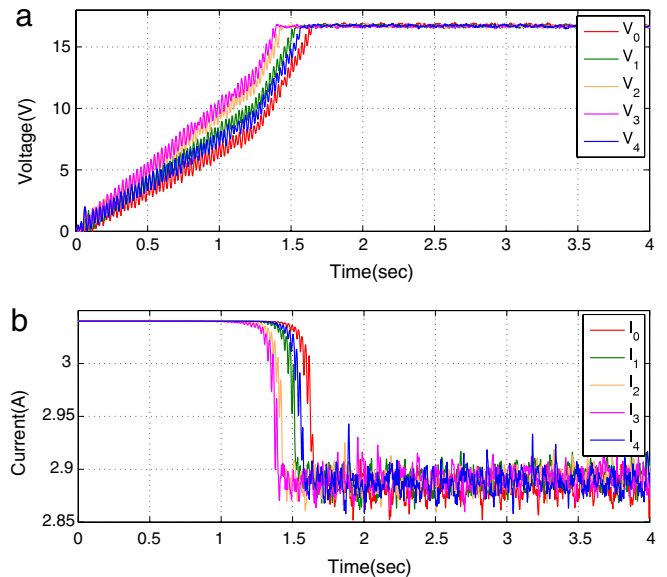


Fig. 12. (a) The corresponding voltages  $V_i$ , ( $i = 0, 1, 2, 3, 4$ ); (b) the corresponding currents  $I_i$ , ( $i = 0, 1, 2, 3, 4$ ).

According to the integral properties, one has

$${}_0D_t^q \text{sgn}(e(t)) = \frac{[f_0(t) + f_1(t) + \dots + f_k(t)]}{\Gamma(1 - q)}, \quad (A.1)$$

where  $f_i(t) = \frac{d}{dt} \int_{t_i}^{t_{i+1}} \frac{\text{sgn}(e(\tau))}{(t-\tau)^q} d\tau$ , ( $i = 0, 1, 2, \dots, k-1$ ),  $f_k(t) = \frac{d}{dt} \int_{t_k}^t \frac{\text{sgn}(e(\tau))}{(t-\tau)^q} d\tau$ .

First of all, we consider the first case  $e(t) > 0$ . Hence,  $e(t') \geq 0$ ,  $\forall t' \in (t_k, t_{k+1}]$  from the above analysis. Let  $t_{k0} = t_k$ ,  $t_{klk} = t$ , one can obtain  $(t_k, t] = (t_{k0}, t_{k1}] \cup (t_{k1}, t_{k2}] \cup \dots \cup (t_{klk-1}, t_{klk}]$ , where if  $e(t') \equiv 0$ ,  $\forall t' \in [t_{ki}, t_{ki+1}]$ ,  $e(t') \geq 0$ ,  $\forall t' \in (t_{ki+1}, t_{ki+2}]$  in which  $e(t') = 0$  just happens at an isolate point  $t'$ . Since

$e(t) > 0$ ,  $e(t') \geq 0$ ,  $\forall t' \in (t_{klk-1}, t_{klk}]$ . Thus, one has

$$\begin{aligned} \frac{d}{dt} \int_{t_{klk-1}}^t \frac{\text{sgn}(e(\tau))}{(t-\tau)^q} d\tau &= (t - t_{klk-1})^{-q}, \\ \frac{d}{dt} \int_{t_{klk-2}}^{t_{klk-1}} \frac{\text{sgn}(e(\tau))}{(t-\tau)^q} d\tau &= \frac{d}{dt} \int_{t_{klk-2}}^{t_{klk-1}} \frac{0}{(t-\tau)^q} d\tau = 0, \\ \frac{d}{dt} \int_{t_{klk-3}}^{t_{klk-2}} \frac{\text{sgn}(e(\tau))}{(t-\tau)^q} d\tau &= \frac{d}{dt} \int_{t_{klk-3}}^{t_{klk-2}} \frac{1}{(t-\tau)^q} d\tau \\ &= (t - t_{klk-3})^{-q} - (t - t_{klk-2})^{-q}, \end{aligned}$$





### Appendix C. Proof of Theorem 2

(i) Attractiveness of  $D_\delta$ : Suppose that  $\theta \notin D_\delta, \forall t \in [0, t_M)$ . From Theorem 1,  $\exists t_f$  such that  $\dot{\tau} = 0$ . Hence,  $\dot{e} = -(\gamma_2/\gamma_1)_0 D_t^\alpha \text{sgn}(e), \forall t \geq t_f$ . From Lemma 2,  $y_r$  draws  $y$  close in  $y^*$ . Since  $y \leq y^*$  and  $y_r$  strictly increases with time,  $y_r > y^* \geq y$  and  $e < 0$  for large enough  $t$ . So  $y$  increases with  $\dot{y} = k_r - (\gamma_2/\gamma_1)_0 D_t^\alpha \text{sgn}(e) > 0$  for large enough  $t$ , i.e.  $y = F(\theta)$  must be close to  $y^*$ . So,  $\theta$  approaches  $D_\delta$ , which is a contradiction. Thus,  $D_\delta$  is accomplished in finite time. Thus,  $\theta$  remains or oscillates around  $D_\delta$ . Hence,  $y$  stays in or oscillates around some small vicinity of  $y^*$ . These oscillations appear due to the recurrent changes in the sign of  $F'$  at the vicinity of  $(\theta^*, y^*)$  where  $F' = 0$ . Meantime,  $\tau$  can switch from one sliding surface  $\tau = l\gamma_0$  (odd number  $l$  ( $\text{sgn}(k) > 0$ )) to another surface (even number  $l$  ( $\text{sgn}(k) < 0$ )). Since  $y$  could start oscillations around  $y^*$  with increasing maximum amplitude, it should prove that  $|y - y^*|$  can be made ultimately of order  $O(\gamma_0)$ .

(ii) Oscillations of order  $O(\gamma_0)$  around  $y^*$ : From Assumption 3, if  $\theta$  stays in  $D_\delta, \forall t$ , one has  $|y - y^*| = O(\gamma_0)$ . Next, it will illustrate that  $|y - y^*| = O(\gamma_0)$  when  $\theta$  oscillates around  $D_\delta$ . One has  $y_r > y^* \geq y, \forall t$  large enough. Thus,  $\exists \tilde{t} > 0$  such that  $e(t) < 0, \forall t > \tilde{t}$ . From Lemma 2,  $_0 D_t^\alpha \text{sgn}(e) < 0, \forall t > \tilde{t}$ . One has  $\tau(t) = \gamma_1 y(t) - \gamma_1 y_r(t) + \gamma_2 ({}_0 D_t^{\alpha-1} \text{sgn}(e))$ . Suppose that  $\theta$  arrives at  $D_\delta$  from inside at  $\tilde{t}_1 > \tilde{t}$  and  $\tau(t)$  is not in sliding surface when  $t = \tilde{t}_1$ .  $D_\delta$  is constant when  $\tau(t)$  is in sliding manifold. Define  $\tilde{\tau}(t) = \tau(t) - \tau(\tilde{t}_1), \tilde{y}(t) = y(t) - y(\tilde{t}_1)$ , one has

$$\tilde{\tau}(t) = \gamma_1 \tilde{y}(t) - \gamma_1 k_r (t - \tilde{t}_1) + \gamma_2 ({}_0 D_t^{\alpha-1} \text{sgn}(e)). \quad (C.1)$$

From Lemma 1,  $\exists K > 0$  such that  $|{}_0 D_t^{\alpha-1} \text{sgn}(e)| < K|\text{sgn}(e)| = K$ . Hence, one has  $|\tilde{y}(t)| \leq \gamma_1 |\tilde{\tau}(t)| + \gamma_1 k_r (t - \tilde{t}_1) + K$ . Let  $\tilde{t}_2$  be the first time when  $\tau(t)$  arrives at the next sliding surface  $\tau(t) = \tau(\tilde{t}_2)$  and  $\tilde{t}_3$  is the first time when  $\theta$  reaches the frontier of  $D_\delta$  again (from outside). One has  $\tilde{t}_2 \geq \tilde{t}_1, \tilde{t}_3 \geq \tilde{t}_1$ . Then, consider two cases: (I)  $\tilde{t}_3 \leq \tilde{t}_2$  and (II)  $\tilde{t}_3 > \tilde{t}_2$ .

For (I), let  $t \in [\tilde{t}_1, \tilde{t}_2)$ .  $\tau(t)$  is not in sliding manifold during  $[\tilde{t}_1, \tilde{t}_2)$ . Hence,  $\exists$  some integer  $l$  such that  $l\gamma_0 < \tau(t) < (l+1)\gamma_0$ . Otherwise, sliding mode happens in  $\tau(t) = l\gamma_0$  or  $\tau(t) = (l+1)\gamma_0$ . Hence,  $|\tilde{\tau}(t)| = |\tau(t) - \tau(\tilde{t}_1)| = O(\gamma_0), \forall t \in [\tilde{t}_1, \tilde{t}_2)$ . Since  $0 < |\tanh(\sin(\pi\tau(t)/\gamma_0))| \leq 1, \forall t \in [\tilde{t}_1, \tilde{t}_2)$ , one has  $|v(t)| \geq |\phi \tanh^2(\sin(\pi\tau(t)/\gamma_0))|$ . They guarantee  $\alpha > 0$  so that  $|\dot{\tau}(t)| \geq \tilde{\alpha}(|\phi \tanh^2(\sin(\pi\tau(t)/\gamma_0))| - |\omega|) \geq \tilde{\alpha}$  in which  $\tilde{\alpha} = \tilde{\kappa}\alpha > 0$ . Thus,  $(t - \tilde{t}_1) \leq |\tilde{\tau}|/\tilde{\alpha}, \forall t \in [\tilde{t}_1, \tilde{t}_2)$  and  $(t - \tilde{t}_1)$  is of order  $O(\gamma_0), \forall t \in [\tilde{t}_1, \tilde{t}_2)$ . Thus, one can assure that  $y(t) - y(\tilde{t}_1)$  is of order  $O(\gamma_0), \forall t \in [\tilde{t}_1, \tilde{t}_2)$ . By continuity,  $|y(t) - y(\tilde{t}_1)| = O(\gamma_0), \forall t \in [\tilde{t}_1, \tilde{t}_2)$ .

For (II), let  $t \in [\tilde{t}_1, \tilde{t}_3]$ . Therefore, we have that  $y(t) - y(\tilde{t}_1)$  is of order  $O(\gamma_0), \forall t \in [\tilde{t}_1, \tilde{t}_2)$ . Next, consider  $t \in [\tilde{t}_2, \tilde{t}_3]$ . Since  $\tau(t)$  is in sliding motion during  $[\tilde{t}_2, \tilde{t}_3]$ , one has  $\dot{\tau}(t) = 0, y(t) = 0, \forall t \in [\tilde{t}_2, \tilde{t}_3]$  is increasing with  $\dot{y} = k_r - (\gamma_2/\gamma_1)_0 D_t^\alpha \text{sgn}(e) > 0$ . Hence,  $y(t)$  continues to approach  $y^*$  during  $[\tilde{t}_2, \tilde{t}_3]$ . So,  $y(t) - y(\tilde{t}_1)$  is of order  $O(\gamma_0), \forall t \in [\tilde{t}_2, \tilde{t}_3]$ . One has that the oscillation outside  $D_\delta$  is of order  $O(\gamma_0), \forall t \in [\tilde{t}_1, \tilde{t}_3]$ . The boundedness of  $y$  means that  $\theta$  is UB, from the continuity of  $y = F(\theta)$ . Although  $\lim_{t \rightarrow +\infty} |\tau(t)| = +\infty$  (actually, it is just an argument of an FO sign function in (5)), it is not bad for UB of other signals. One can derive that other closed-loop signals are UB.

### References

- Ariyur, K. B., & Krstić, M. (2003). *Real-time optimization by extremum-seeking control*. Wiley-Blackwell.
- Cochran, J., & Krstić, M. (2007). Source seeking with a nonholonomic unicycle without position measurements and with tuning of angular velocity part I: stability analysis. In *Proceedings of the 46th IEEE conference on decision and control* (pp. 6009–6016). IEEE.

- DeHaan, D., & Guay, M. (2005). Extremum-seeking control of state-constrained nonlinear systems. *Automatica*, 41(9), 1567–1574.
- Drakunov, S., Özgüner, Ü, Dix, P., & Ashrafi, B. (1995). ABS control using optimum search via sliding modes. *IEEE Transactions on Control Systems Technology*, 3(1), 79–85.
- Fu, L., & Özgüner, Ü (2011). Extremum seeking with sliding mode gradient estimation and asymptotic regulation for a class of nonlinear systems. *Automatica*, 47(12), 2595–2603.
- Kilbas, A. A., Srivastava, H. M., & Trujillo, J. J. (2006). *Theory and applications of fractional differential equations*. Amsterdam, Netherlands: Elsevier.
- Krstić, M., & Wang, H. H. (2000). Stability of extremum seeking feedback for general nonlinear dynamic systems. *Automatica*, 36(4), 595–601.
- Luo, Y., & Chen, Y. Q. (2012). Stabilizing and robust fractional order PI controller synthesis for first order plus time delay systems. *Automatica*, 48(2), 2159–2167.
- Malek, H., Dadras, S., & Chen, Y. Q. (2012). A fractional order maximum power point tracker: stability analysis and experiments. In *Proceedings of the 51th IEEE conference on decision and control* (pp. 6861–6866). IEEE.
- Monje, C. A., Chen, Y. Q., Vinagre, B. M., Xue, D., & Feliu, V. (2010). *Fractional-order systems and controls: fundamentals and applications*. Springer.
- Oliveira, T. R., Hsu, L., & Peixoto, A. J. (2011). Output-feedback global tracking for unknown control direction plants with application to extremum-seeking control. *Automatica*, 47(9), 2029–2038.
- Oliveira, T. R., Peixoto, A. J., & Hsu, L. (2012). Global real-time optimization by output-feedback extremum-seeking control with sliding modes. *Journal of the Franklin Institute*, 349, 1397–1415.
- Pan, Y., Özgüner, Ü, & Acarman, T. (2003). Stability and performance improvement of extremum seeking control with sliding mode. *International Journal of Control*, 76(9–10), 968–985.
- Podlubny, I. (1999). Fractional-order systems and  $P^i D^{\mu}$ -controllers. *IEEE Transactions on Automatic Control*, 44(1), 208–214.
- Popovic, D., Jankovic, M., Magner, S., & Teel, A. R. (2006). Extremum seeking methods for optimization of variable cam timing engine operation. *IEEE Transactions on Control Systems Technology*, 14(3), 398–407.
- Samko, S. G., Kilbas, A. A., & Marichev, O. I. (1993). *Fractional integrals and derivatives: theory and applications*. Switzerland: Gordon and Breach Science Publishers.
- Tan, Y., Nešić, D., & Mareels, I. (2006). On non-local stability properties of extremum seeking control. *Automatica*, 42(6), 889–903.
- Tarte, Y., Chen, Y. Q., Ren, W., & Moore, K. (2006). Fractional horsepower dynamometer—a general purpose hardware-in-the-loop real-time simulation platform for nonlinear control research and education. In *Proceedings of the 45th IEEE conference on decision and control* (pp. 3912–3917). IEEE.
- Teel, A. R., & Popović, D. (2001). Solving smooth and nonsmooth multivariable extremum seeking problems by the methods of nonlinear programming. In *Proceedings of the 2001 American control conference*. Vol. 3 (pp. 2394–2399). IEEE.
- Walker, G. (2001). Evaluating MPPT converter topologies using a MATLAB PV model. *Journal of Electrical and Electronics Engineering, Australia*, 21(1), 49–56.
- Yin, C., Stark, B., Chen, Y. Q., & Zhong, S. M. (2013). Adaptive minimum energy cognitive lighting control: integer order vs. fractional order strategies in sliding mode based extremum seeking. *Mechatronics*, 23(7), 863–872.
- Yin, C., Stark, B., Zhong, S., & Chen, Y. Q. (2012). Global extremum seeking control with sliding modes for output-feedback global tracking of nonlinear systems. In *Proceedings of the 51th IEEE conference on decision and control* (pp. 7113–7118). IEEE.
- Zhang, C., & Ordóñez, R. (2009). Robust and adaptive design of numerical optimization-based extremum seeking control. *Automatica*, 45(3), 634–646.



**Chun Yin** received the Ph.D. degree from School of Mathematics Science, University of Electronic Science and Technology of China, Chengdu, China in 2014. She was an exchange Ph.D. student from 2011 to 2012 in the Center for Self-Organizing and Intelligent Systems, department of Electrical and Engineering at Utah State University, Logan, UT, USA. She was an exchange Ph.D. student from 2012 to 2013 in MESA Lab, University of California, Merced, CA, USA. Her research interests include fractional order extremum seeking control, fractional-order sliding mode control, stability theorem, and cognitive control.



**YangQuan Chen** received B.S. in industrial automation from University of Science and Technology, Beijing, China in 1985, M.S. in automatic control from the Beijing Institute of Technology, Beijing, China in 1989, and the Ph.D. degree in advanced control and instrumentation from the Nanyang Technological University, Singapore, in 1998. He is currently an Associate Professor of University of California, Merced and the Director of MESA Lab (Mechatronics, Embedded Systems and Automation). From 2010 to 2012, he had been with the Center for Self-Organizing and Intelligent Systems (CSOIS), Dept. of Electrical and Computer Engineering, Utah State University. His current areas of research interest include:



applied fractional calculus in controls, signal processing and energy informatics; distributed measurement and distributed control of distributed parameter systems using mobile actuator and sensor networks; mechatronics; multi-UAV based cooperative multi-spectral “personal remote sensing” for precision agriculture and environmental monitoring. He is an Associate Editor for Acta Montanistica Slovaca, IFAC journal Mechatronics, Fractional Calculus and Applied Analysis, ASME Journal of Dynamical Systems, Measurement and Control, IEEE Transactions of Control Systems Technology, ISA Transactions, IFAC Journal Control Engineering Practice. He serves as the Topic-Editor-in-Chief in “Field Robotics” for International Journal of Advanced Robotic Systems, a Founding Associate Editor for Unmanned Systems and a Senior Editor for International Journal of Intelligent and Robotic Systems.



**Shou-ming Zhong** was born on November 5, 1955. He graduated from University of Electronic Science and Technology of China, majoring in applied mathematics on differential equation. He has been a professor in the School of Mathematical Sciences, University of Electronic Science and Technology of China since June 1997. He is the Director of Chinese Mathematical Biology Society, the Chair of Biomathematics in Sichuan Province, and an Editor of Journal of Biomathematics. His research interests are in stability theorem and its application of the differential system, robustness in control, neural network

and Biomathematics.